

New approach to the $\mathbf{k} \cdot \mathbf{p}$ theory of semiconductor superlattices^{a)}

C. Mailhot,^{b)} T. C. McGill, and D. L. Smith^{c)}

T. J. Watson, Sr., Laboratory of Applied Physics, California Institute of Technology, Pasadena, California 91125

(Received 30 January 1984; accepted 17 April 1984)

Along with the growing interest in semiconductor superlattices, various theoretical schemes have been proposed to study the nature of the electronic states within these structures. The work presented here highlights a new method to investigate the electronic and optical properties of semiconductor superlattices. The backbone of the theory rests on a realistic description of the complex- \mathbf{k} band structure of the constituent semiconductors coupled with a suitable set of boundary conditions for the superlattice wave function. The bulk Bloch solutions, propagating and evanescent, in each semiconductor are described within a full-zone $\mathbf{k} \cdot \mathbf{p}$ Hamiltonian that provides an accurate description of the solutions up to the first Brillouin zone edge. An attractive feature of the present treatment is that the complex- \mathbf{k} bulk Bloch solutions of *each constituent semiconductor* are expanded on the *same set of zone-center basis functions*. A new technique for constructing the $\mathbf{k} \cdot \mathbf{p}$ Hamiltonian of each constituent semiconductor is presented. The superlattice wave function is described by a linear combination of propagating and evanescent bulk Bloch solutions. The expansion amplitudes are determined by imposing a set of boundary conditions on the superlattice wave function across the superlattice interfaces. These boundary conditions are used to formulate an eigenvalue problem whose solution yields directly the corresponding superlattice states associated with real or complex superlattice wave vector \mathbf{q} . This method provides an accurate technique to treat superlattices where one of the constituent semiconductors has an indirect energy band gap. An exposition of the formalism is presented, and the physical origin of the superlattice states is studied. The test case of the GaAs-AlAs (100) superlattice is presented. Pertinent applications are also discussed.

PACS numbers: 71.25.Tn, 73.40.Lq, 71.10. + x, 78.20.Bh

I. INTRODUCTION

Superlattice structures are made by the alternate deposition of layers of two lattice-matched solids. Semiconductor superlattices can be viewed as completely new materials whose electronic and optical properties are not just a combination of the properties of the bulk constituent semiconductors. In fact, it is possible to tailor the electronic and optical properties of semiconductor superlattices over a large range.¹ It is this flexibility that makes semiconductor superlattices vastly more interesting than the corresponding semiconductor alloys, regarding certain applications.

The *optical properties* of quantum well structures and semiconductor superlattices have generated a lot of experimental work in the past few years. More specifically, the fabrication of *quantum well lasers*² has opened a totally new area of applications. In the light of these new applications, it is imperative to devise a theory that allows for a deeper understanding of the optical properties of semiconductor superlattices. This paper is devoted to the presentation of a novel and general formalism well suited for the study of the optical properties of semiconductor superlattices. The formalism presented here will serve as a basis for future studies in the area of the optical properties of semiconductor superlattices.

This paper is concerned with the study of the electronic structure of semiconductor superlattices. The first step leading to realistic superlattice electronic structures is the accurate calculation of the electronic band structure of the con-

stituent semiconductors. The following procedure allows us to describe the constituent semiconductors in terms of the *same set of basis functions* associated with $\mathbf{k}_0 = 0$ through the use of local pseudopotentials.

We now outline the theoretical method used. The local pseudopotential Hamiltonian of each semiconductor forming the superlattice is expressed in terms of a local pseudopotential Hamiltonian associated with a *reference solid*. We then operate a transformation on the local pseudopotential Hamiltonian of each solid in order to transform from a plane wave representation, to a representation in terms of $\mathbf{k}_0 = 0$ basis functions associated with the *same* reference solid. We refer to this representation as the $\mathbf{k} \cdot \mathbf{p}$ representation. Within the $\mathbf{k} \cdot \mathbf{p}$ formalism, all the bulk Bloch solutions, propagating and evanescent, are obtained.

The superlattice state function is then expanded in terms of propagating and evanescent Bloch solutions in each solid, expressed in terms of the *same set of basis functions associated with $\mathbf{k}_0 = 0$* . The expansion coefficients are the *multicomponent envelope functions*. A suitable set of boundary conditions on the superlattice wave function, formulated in terms of an eigensystem, allows us to calculate the envelope function. The major feature of this work is that the set $\mathbf{k}_0 = 0$ basis functions on which the superlattice wave function is expanded is *the same in both solids*. This is done by explicit *construction* from pseudopotentials and not by *assumption* as was done in previous work.³ We therefore relieve any ambiguity in the matching conditions for the superlattice wave function across the interfaces.

The paper is organized as follows: in Sec. II the theoretical method is developed in a general fashion. An application to the case of the GaAs–AlAs(100) superlattice is presented and discussed in Sec. III. A summary and conclusions are given in Sec. IV.

II. THEORY

In this section, we develop the major theoretical components to the calculation of the electronic structure of semiconductor superlattices. We discuss first the procedure by which we construct the pseudopotential Hamiltonian of the reference solid. Then we indicate how the transformation from the set of plane waves to the set of $\mathbf{k}_0 = 0$ basis functions is operated so as to provide the grounds for the $\mathbf{k} \cdot \mathbf{p}$ formulation.

A. Local pseudopotential and $\mathbf{k} \cdot \mathbf{p}$

We now give the prescription on how to construct the local pseudopotential Hamiltonian of the reference solid corresponding to the two constituent semiconductors forming the superlattice.

We express the Hamiltonian $H^{(j)}(\mathbf{g}\mathbf{g}';\mathbf{k})$ of each constituent solid $j = 1, 2$ in terms of a common Hamiltonian $H^{(0)}(\mathbf{g}\mathbf{g}';\mathbf{k})$ associated with a reference solid. Let us take the reference Hamiltonian $H^{(0)}(\mathbf{g}\mathbf{g}';\mathbf{k})$ to be the average of the local pseudopotential Hamiltonians $H^{(j)}(\mathbf{g}\mathbf{g}';\mathbf{k})$ in each solid. The Hamiltonian of solid $j = 1, 2$ can then be written as a sum of the reference Hamiltonian $H^{(0)}(\mathbf{g}\mathbf{g}';\mathbf{k})$ plus a perturbation term $\Delta V^{(j)}(\mathbf{g} - \mathbf{g}')$. The perturbation pseudopotential form factor $\Delta V^{(j)}(\mathbf{g})$ contains a symmetric part $\Delta V^{(j,S)}(\mathbf{g})$ and an antisymmetric part $\Delta V^{(j,A)}(\mathbf{g})$.

We now transform from the pseudopotential formalism to the $\mathbf{k} \cdot \mathbf{p}$ formalism. Let $\{|m\rangle\}$ be the set of $\mathbf{k}_0 = 0$ basis functions associated with the reference solid and let $\{|\mathbf{g}\rangle\}$ be the set of plane waves corresponding to the reciprocal lattice vectors \mathbf{g} . The transformation matrix $U(\mathbf{g}, m)$ that allows the transformation from the $\{|\mathbf{g}\rangle\}$ representation to the $\{|m\rangle\}$ representation is the eigenvector matrix that diagonalizes the local pseudopotential Hamiltonian of the reference solid at $\mathbf{k}_0 = 0$.

We now express the Hamiltonian of the solids $j = 1, 2$ in the $\{|m\rangle\}$ representation. We can write explicitly,

$$H^{(j)}(mm';\mathbf{k}) \equiv \left[E_m(0) + \frac{\hbar^2}{2m} \mathbf{k}^2 \right] \delta(m, m') + \frac{\hbar \mathbf{k}}{m} \langle m | \mathbf{p} | m' \rangle + \Delta V^{(j)}(mm'), \quad (1a)$$

where the perturbation potential in the $\{|m\rangle\}$ representation is

$$\Delta V^{(j)}(mm') = \sum_{\mathbf{g}} \sum_{\mathbf{g}'} [U(\mathbf{g}, m)]^\dagger \Delta V^{(j)}(\mathbf{g} - \mathbf{g}') U(\mathbf{g}', m') \quad (1b)$$

and where $E_m(0)$ is the energy of the state $|m\rangle$ of the reference solid at $\mathbf{k}_0 = 0$. In a $\{|m\rangle\}$ representation in which the reference Hamiltonian $H^{(0)}(mm';\mathbf{k})$ is diagonal at $\mathbf{k}_0 = 0$, the Hamiltonian of solid j contains a nondiagonal perturbation term $\Delta V^{(j)}(mm')$.

We again stress the fact that since the zone-center basis functions $\{|m\rangle\}$ are *constructed* to be the same in each solid forming the superlattice, there is no possible ambiguity when the superlattice wave function is matched across the interfaces. A simplified two-band $\mathbf{k} \cdot \mathbf{p}$ model that takes into account the different nature of $\mathbf{k}_0 = 0$ basis functions has been used by Sai-Halasz *et al.*⁴ Furthermore, the number N of basis functions $\{|m\rangle\}$ included is large enough to provide an accurate and convergent description of the electronic structure of each of the constituent solid up to the Brillouin zone edge by retaining basis functions of atomic symmetry s, p, d , and f . This is necessary when one of the constituent semiconductor has an indirect band gap.

B. Superlattice wave function

Let $\hat{\mathbf{z}}$ be the direction normal to the superlattice interfaces. The set of Bloch states, propagating and evanescent $\{|\mathbf{k}_\parallel E; k_\lambda^{(j)}\rangle\}$ are solutions of the bulk Schrödinger equation in solid j . Here, $\lambda = 1, \dots, 2N$ labels the real and complex solutions $\hat{\mathbf{z}} k_\lambda^{(j)}$ for a given parallel wave vector \mathbf{k}_\parallel and total energy E . The propagating and evanescent bulk Bloch solutions $|\mathbf{k}_\parallel E; k_\lambda^{(j)}\rangle$ in both solids can be expanded in terms of the *same* set of N basis functions $\{|m\rangle\}$ of a reference solid as

$$|\mathbf{k}_\parallel E; k_\lambda^{(j)}\rangle = \exp(i\mathbf{k}_\parallel \cdot \mathbf{x}_\parallel) \exp(ik_\lambda^{(j)} z) \times \sum_{m=1}^N |m\rangle C^{(j)}(m, k_\lambda^{(j)}; \mathbf{k}_\parallel E), \quad (2)$$

where \mathbf{x}_\parallel is a position vector in the plane of the interface. The expansion coefficients $C^{(j)}(m, k_\lambda^{(j)}; \mathbf{k}_\parallel E)$ can be calculated through direct diagonalization of a *companion matrix* related to the $\mathbf{k} \cdot \mathbf{p}$ Hamiltonian matrix.⁵ The calculation of the complex- \mathbf{k} energy eigensolutions, within the full-zone $\mathbf{k} \cdot \mathbf{p}$ formalism, was first performed by Chaves *et al.*⁶ They restricted their study to pure imaginary k_λ solutions.

Let the superlattice state at fixed parallel wave vector \mathbf{k}_\parallel and energy E in solid j be $|\mathbf{k}_\parallel E; \mathbf{q}; j\rangle$, where \mathbf{q} is the superlattice wave vector that labels the superlattice states. We now expand the superlattice state $|\mathbf{k}_\parallel E; \mathbf{q}; j\rangle$ on the set of propagating and evanescent Bloch solutions $\{|\mathbf{k}_\parallel E; k_\lambda^{(j)}\rangle\}$ in each solid:

$$|\mathbf{k}_\parallel E; \mathbf{q}; j\rangle = \sum_{\lambda=1}^{2N} |\mathbf{k}_\parallel E; k_\lambda^{(j)}\rangle \cdot f^{(j)}(k_\lambda^{(j)}; \mathbf{q}; \mathbf{k}_\parallel), \quad (3)$$

where the amplitudes $f^{(j)}(k_\lambda^{(j)}; \mathbf{q}; \mathbf{k}_\parallel)$ indicate the admixture of the bulk solutions $|\mathbf{k}_\parallel E; k_\lambda^{(j)}\rangle$ in the superlattice state $|\mathbf{k}_\parallel E; \mathbf{q}; j\rangle$. Since the bulk Bloch solutions in both solids are described in a zone-center expansion set $\{|m\rangle\}$ associated with a common reference solid, the superlattice state can, in turn, be expressed as a linear combination of zone-center basis functions $\{|m\rangle\}$ of the reference solid. By using explicitly an \mathbf{x} representation, we can write

$$\langle \mathbf{x} | \mathbf{k}_\parallel E; \mathbf{q}; j \rangle \equiv \sum_{m=1}^N \langle \mathbf{x} | m \rangle F^{(j)}(m; \mathbf{k}_\parallel \mathbf{q}; \mathbf{x}), \quad (4)$$

where the functions $F^{(j)}(m; \mathbf{k}_\parallel \mathbf{q}; \mathbf{x})$ associated with the basis function $|m\rangle$ are referred to as *multicomponent envelope functions* and are defined as:

$$F^{(\lambda)}(m; \mathbf{k}_{\parallel}, \mathbf{q}; \mathbf{x}) \equiv \exp(i\mathbf{k}_{\parallel} \cdot \mathbf{x}_{\parallel}) \times \sum_{\lambda=1}^{2N} [\exp(ik_{\lambda}^{(\lambda)} z) C^{(\lambda)}(m, k_{\lambda}^{(\lambda)}; \mathbf{k}_{\parallel}, E)] f^{(\lambda)}(k_{\lambda}^{(\lambda)}; \mathbf{q}; \mathbf{k}_{\parallel}). \quad (5)$$

The amplitudes $f^{(\lambda)}(k_{\lambda}^{(\lambda)}; \mathbf{q}; \mathbf{k}_{\parallel})$ are determined by application of a suitable set of boundary conditions on the superlattice wave function. In the present work, we proceeded as follows:

(i) The local pseudopotential Hamiltonian of the reference solid is constructed.

(ii) From the transformation that diagonalizes the pseudopotential Hamiltonian of the reference solid at $\mathbf{k}_0 = 0$, the Hamiltonian is transformed from the $\{| \mathbf{g} \rangle\}$ representation of the pseudopotential to the $\{| m \rangle\}$ representation of the $\mathbf{k} \cdot \mathbf{p}$. The $\mathbf{k} \cdot \mathbf{p}$ Hamiltonian of both solids forming the superlattice is thus expressed in terms of the same set of $\mathbf{k}_0 = 0$ basis functions $| m \rangle$ of a reference solid. At this point, the $\mathbf{k} \cdot \mathbf{p}$ Hamiltonian is truncated to include $N = 27$ basis functions $| m \rangle$ associated with $\mathbf{k}_0 = 0$. By taking 27 zone-center basis functions, we include states of atomic symmetries s, p, d and f . This is necessary in order to provide a convergent description of the bulk Bloch solutions at the edge of the Brillouin zone.

(iii) The complex- \mathbf{k} band structure is obtained from this truncated $\mathbf{k} \cdot \mathbf{p}$ Hamiltonian. This produces $2N = 54$ solutions $k_{\lambda}^{(\lambda)}$ corresponding to the propagating and evanescent Bloch states $|\mathbf{k}_{\parallel}, E; k_{\lambda}^{(\lambda)}\rangle$.

C. Boundary conditions and superlattice band structure

We now indicate how the complex- \mathbf{q} band structure of the superlattice can be calculated by the application of boundary conditions on the superlattice wave function $|\mathbf{k}_{\parallel}, E; \mathbf{q}; j\rangle$. Let \mathbf{R} be the superlattice period. We require that the superlattice wave function and its normal derivative be continuous across the superlattice interfaces and satisfy the Bloch theorem. As pointed out by White and Sham³ in order to satisfy the boundary conditions for the superlattice wave function and its derivative, the number of Bloch solutions to be matched must be twice the number of $\mathbf{k}_0 = 0$ basis functions $\{| m \rangle\}$. The kinetic energy term in the $\mathbf{k} \cdot \mathbf{p}$ Hamiltonian has to be retained in order to match a sufficient number of propagating and evanescent bulk Bloch solutions at the interfaces.

It is possible to transform the set of boundary conditions into an eigensystem whose eigenvalues are the Bloch factors $\exp(i\mathbf{q} \cdot \mathbf{R})$ and whose eigenvectors are the amplitudes $f^{(\lambda)}(k_{\lambda}^{(\lambda)}; \mathbf{q}; \mathbf{k}_{\parallel})$ of the multicomponent envelope function $F^{(\lambda)}(m; \mathbf{k}_{\parallel}, \mathbf{q}; \mathbf{x})$. Computational details will be presented elsewhere.⁷

III. RESULTS

In this section, we present some results obtained from the above formalism to the case of the GaAs-AlAs(100) superlattice.

A. Complex- \mathbf{k} bulk band structure: $\mathbf{k} \cdot \mathbf{p}$ theory

We first analyze the complex- \mathbf{k} band structure of bulk GaAs and AlAs. Figures 1 and 2 show a complex- \mathbf{k} energy

band structure for GaAs and AlAs, respectively, as obtained by the 27-band $\mathbf{k} \cdot \mathbf{p}$ method outlined above. Spin-orbit interactions are neglected. The complex- \mathbf{k} band structure corresponds to vanishing wave vector parallel to the (100) interface, i.e., $\mathbf{k}_{\parallel} = 0$. At a given energy E , the purely real values of k_z are indicated by a solid line on the right panel of the figure and the purely imaginary values of k_z are indicated by a solid line on the left panel of the figure. Complex values of k_z are indicated by a dashed line, $\text{Re}[k_z]$ being on the right and $\text{Im}[k_z]$ being on the left of the figure, respectively. The origin of the energies is taken at the top of the GaAs valence band. The maximum of the AlAs valence band is therefore shifted down by the valence band offset,⁸

$$\Delta E_v = 0.15 [E_{\text{gap}}^{\text{AlAs}}(\Gamma) - E_{\text{gap}}^{\text{GaAs}}(\Gamma)]. \quad (6)$$

The band structures shown in Figs. 1 and 2 are obtained from a local pseudopotential calculation including 113 plane waves. The pseudopotential form factors are those of Ref. 9. The $\mathbf{k} \cdot \mathbf{p}$ Hamiltonian is truncated down to include $N = 27$ basis functions $| m \rangle$, thereby retaining basis functions having

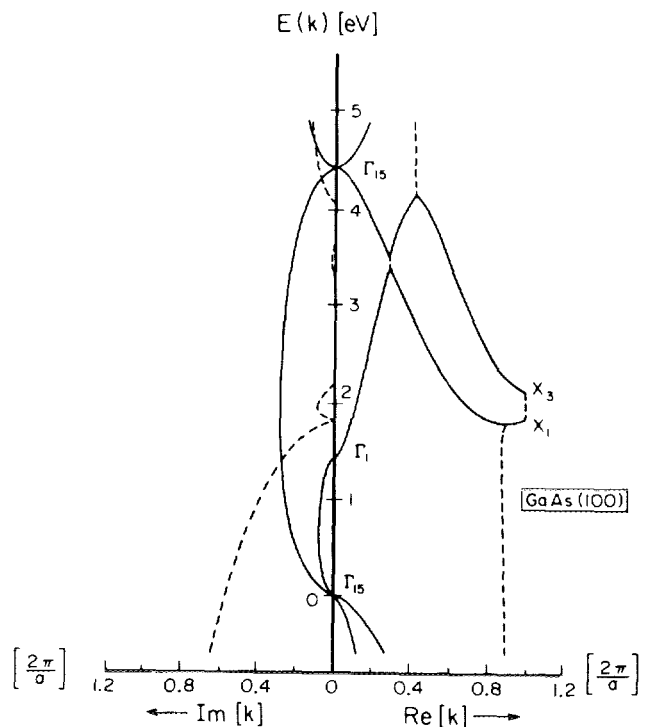


FIG. 1. Complex- \mathbf{k} band structure of GaAs along the (100) direction. Only the energy bands within the first Brillouin zone are shown. The complex- \mathbf{k} band structure corresponds to vanishing wave vector parallel to the (100) interface plane, i.e., $\mathbf{k}_{\parallel} = 0$. At a given energy E , the purely real values of k_z are indicated by a solid line on the right panel of the figure and the purely imaginary values of k_z are indicated by a solid line on the left panel of the figure. Complex values of k_z are indicated by a dashed line, $\text{Re}[k_z]$ being on the right and $\text{Im}[k_z]$ being on the left of the figure, respectively. The zero of energy is taken at the top of the GaAs valence band maximum.

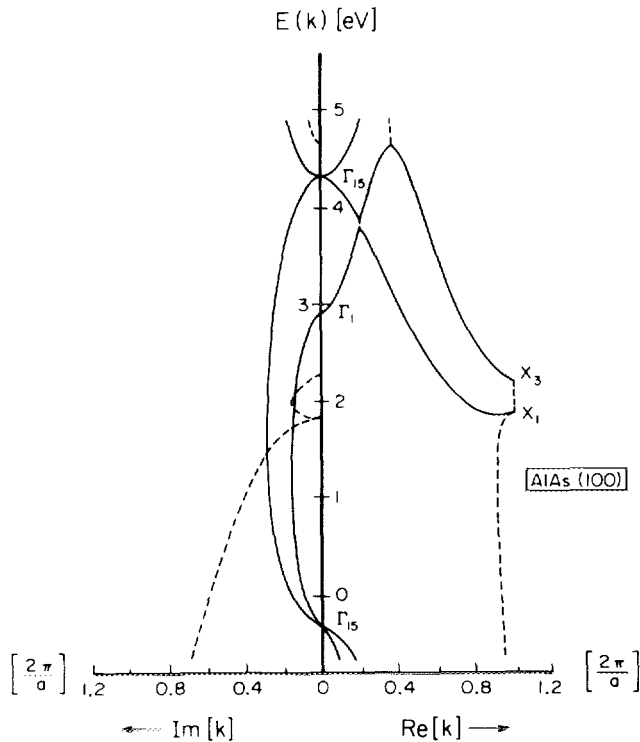


FIG. 2. Complex- k band structure of AlAs along the (100) direction. Only the energy bands within the first Brillouin zone are shown. The complex- k band structure corresponds to vanishing wave vector parallel to the (100) interface plane, i.e., $k_{\parallel} = 0$. At a given energy E , the purely real values of k_z are indicated by a solid line on the right panel of the figure and the purely imaginary values of k_z are indicated by a solid line on the left panel of the figure. Complex values of k_z are indicated by a dashed line, $\text{Re}[k_z]$ being on the right and $\text{Im}[k_z]$ being on the left of the figure, respectively. The zero of energy is taken at the top of the GaAs valence band maximum.

atomic symmetries s, p, d and f . Out of the $2N = 54$ solutions obtained, we only plotted 10 solutions $k_{\lambda}^{(j)}$ whose real part lies within the first Brillouin zone.

The symmetry of the Bloch states at $\mathbf{k}_0 = 0$ and at the Brillouin zone edge are indicated. On the right panel, we can identify, in solid line, the structure at the top of the valence band as well as the two lowest conduction bands. On the left panel, we can identify two major bands for which k_z is pure imaginary. Both of these bands originate from the maximum of the valence band and connect to real bands across the energy gap at $\mathbf{k}_0 = 0$. Within the local pseudopotential scheme used here the $\Gamma_{15}^v - \Gamma_1^c$ energy gap is 1.433 eV for GaAs and 3.205 eV for AlAs. We can also identify complex bands for which both $\text{Re}[k_z]$ and $\text{Im}[k_z]$ are nonvanishing. These bands emanate from the X -point.

B. Superlattice energy gap

We used the procedure described above to study the GaAs-AlAs(100) superlattice. Figure 3 shows the superlattice energy band gap as a function of the number of GaAs monolayers forming the superlattice period. The superlattice period contains 2 monolayers of AlAs and a varying number of GaAs monolayers.

At large GaAs/AlAs ratio, the superlattice state at $\mathbf{q} = 0$ is mostly constructed of bulk Bloch solutions derived from

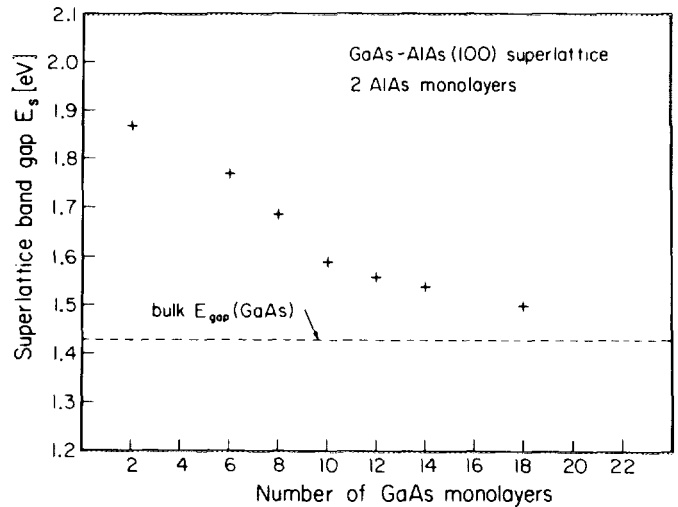


FIG. 3. GaAs-AlAs(100) superlattice energy band gap as a function of the number of GaAs monolayers forming the superlattice period. The superlattice period consists of two monolayers of AlAs.

the Γ point in GaAs and AlAs. These bulk Bloch solutions are propagating ($k_{\lambda}^{\text{GaAs}}$ real) in GaAs and evanescent ($k_{\lambda}^{\text{AlAs}}$ complex) in AlAs. The present scheme provides an accurate description of the decaying character of the wave function in AlAs through the complex- k band structure. As pointed out by Schulman and Chang,¹⁰ in the limit of a large GaAs/AlAs ratio, a simple Kronig-Penney model, a two-band model, and a more complete tight-binding model give a similar description of the superlattice state. At large GaAs/AlAs ratio, the superlattice state function at $\mathbf{q} = 0$ behaves like a particle in a one-dimensional quantum well, and the admixture of bands at higher energy is fairly small.

As the GaAs/AlAs ratio decreases, the contribution from evanescent bulk Bloch solutions emanating from the AlAs X -point increases. The admixture of X -point derived states in the superlattice wave function is accurately described in the present 27-band $k \cdot p$ scheme. As the energy of the $\mathbf{q} = 0$ superlattice state increases towards the X -point minimum of AlAs so does the contribution of the evanescent X -point derived states. At these energies, a simple quantum well picture fails and realistic band structure effects have to be taken into account. Both the present full-zone $k \cdot p$ and the tight-binding models are capable of providing such a realistic description. Simpler models that do not include contribution from the AlAs X -point derived states do not provide that accurate description.

The present scheme is particularly well suited for the evaluation of optical matrix elements since the same set of $\mathbf{k}_0 = 0$ basis functions is used in each solid to describe the superlattice wave function in GaAs and AlAs. Furthermore, in the present $k \cdot p$ scheme the admixture of basis functions of symmetry s, p, d , and f is retained to describe accurately the bulk Bloch solutions at the X point.

IV. SUMMARY AND CONCLUSIONS

We have developed a general formalism for the study of the optical properties of semiconductor superlattices which relaxes the often used approximation¹¹⁻¹² that the $\mathbf{k}_0 = 0$

functions of all the III-V semiconductors are the same. The formalism is essentially based on a local pseudopotential description of the constituent semiconductors. We now summarize the basic ingredients of the theory.

(i) An accurate description of the bulk constituent semiconductors forming the superlattice is obtained via a local pseudopotential description.

(ii) A transformation from the local pseudopotential formalism to the $k \cdot p$ formalism is then performed. At this point, the $k \cdot p$ Hamiltonian of each semiconductor is expressed in terms of the *same set of basis functions* $|m\rangle$ associated with $\mathbf{k}_0 = 0$. This feature is novel and relieves any ambiguity when the superlattice wave function is matched across the interface planes.

(iii) The complex- k energy band structure of each semiconductor is then obtained within the $k \cdot p$ formalism. All the bulk Bloch solutions, associated with real or complex values of k , are therefore expanded in terms of the *same set of zone-center basis functions*. An accurate and convergent description of the electronic structure of each constituent solid is obtained up to the Brillouin zone edge by including zone-center basis functions of atomic symmetry s , p , d , and f . The technique is therefore equally valid when one of the constituent solids has an indirect energy gap.

(iv) The superlattice state function is then expanded in terms of all the bulk Bloch solutions associated with complex k in each solid. A set of boundary conditions is then imposed on the superlattice wave function and formulated in terms of an eigensystem for the expansion amplitudes for the envelope functions. The eigenvalues of this eigensystem are the complex values of q , the superlattice wave vector.

An application to the case of the GaAs-AlAs(100) superlattice indicates that the admixture of X -point derived bulk solutions is properly taken into account in the limit of GaAs/AlAs ratio approaching unity.

^{a1}Work supported in part by Army Research Office under Contract No. DAAG29-80-C-0103 and Office of Naval Research under Contract No. N00014-81-K-0305.

^{b1}Present Address: Xerox Webster Research Center, Webster, N. Y. 14580.

^{c1}Present Address: Los Alamos National Laboratory, Los Alamos, N. M. 87545.

¹G. C. Osbourn, *J. Vac. Sci. Technol. B* **1**, 379 (1983).

²N. Holonyak, Jr., R. M. Kolbas, R. D. Dupuis, and P. D. Dapkus, *IEEE J. Quantum Electron.* **QE-16**, 170 (1980).

³S. R. White and L. J. Sham, *Phys. Rev. Lett.* **47**, 879 (1981).

⁴G. A. Sai-Halasz, R. Tsu, and L. Esaki, *Appl. Phys. Lett.* **30**, 651 (1977).

⁵The companion matrix is associated with the Hamiltonian matrix. We transform the $k \cdot p$ Hamiltonian matrix containing a kinetic energy term in k_z^2 into a matrix which has twice the dimension as the original Hamiltonian matrix but contains only linear terms in k_z . The companion matrix used in the present work is directly related to the boundary condition matrix and the procedure to obtain it will be given elsewhere.

⁶C. M. Chaves, N. Majlis, and M. Cardona, *Solid State Commun.* **4**, 271 (1966).

⁷C. Mailhot, D. L. Smith, and T. C. McGill (to be published).

⁸H. C. Casey, Jr. and M. B. Panish, *Heterostructure Lasers* (Academic, New York, 1978), Part A, Chap. 4.

⁹M. L. Cohen and T. K. Bergstresser, *Phys. Rev.* **141**, 789 (1966).

¹⁰J. N. Schulman and Y. C. Chang, *Phys. Rev. B* **24**, 4445 (1981).

¹¹M. Altarelli, *Phys. Rev. B* **28**, 842 (1983).

¹²G. Bastard, *Phys. Rev. B* **25**, 7584 (1982).